A fluorescence stopped-flow kinetic study of the conformational activation of α-chymotrypsin and several mutants

GERT VERHEYDEN,[1,3] JANKA MATRAI,[1] GUIDO VOLCKAERT,[2] AND YVES ENGELBORGHS[1]

[1]Laboratory of Biomolecular Dynamics and [2]Laboratory of Genetechnolgy, Katholieke Universiteit Leuven, B-3001 Leuven, Belgium

(RECEIVED February 27, 2004; FINAL REVISION June 2, 2004; ACCEPTED June 3, 2004)

Abstract

The kinetic activation parameters (activation free energy, activation free enthalpy, and activation free entropy change) of the conformational change of α-chymotrypsin from an inactive to the active conformation were determined after a pH jump from pH 11.0 to pH 6.8 by the fluorescence stopped-flow method. The conformational change was followed by measuring changes in the protein fluorescence. For the bovine wild-type protein, the same kinetic parameters are obtained as in the study of proflavin binding. Several mutants were made with the goal to accelerate or decelerate this conformational transition. The inspiration for the choice of the mutants came from a previous modelling study done on the bovine wild-type chymotrypsin. The results of the fluorescence stopped flow experiments show that several mutants behaved as was expected based on the information provided by the modeling study on the wild-type variant. For some mutants our assumptions were not correct, and therefore additional modeling studies of the activation pathways of these mutant proteins are necessary to be able to explain the observed kinetic behavior.

Keywords: tryptophan fluorescence; fluorescence stopped-flow measurements; targeted molecular dynamics; structure–function relationship

A detailed understanding of the conformational dynamics of a protein is still a difficult task. Molecular Dynamics (MD) is able to study the dynamic behavior of proteins, but only on the nanosecond time scale in the best case. Many attempts are made to describe the conformational changes and to characterize the important intermediate structures of proteins in the course of their folding, which is usually a much slower process (Berendsen and Hayward 2000). At room temperature, choosing systems containing more than ~100 amino acid residues in the presence of explicit solvent and by trying to keep the simulation time in a reasonable range, for elaborate conformational changes other techniques than Molecular Dynamics Calculations have to be applied, for example, Targeted Molecular Dynamics (TMD; Schlitter et al. 1994; W. Swegat, P. Krueger, and W.J. Rutter, pers. comm.) or Steered Molecular Dynamics (SMD; Izrailev et al. 1998).

Such detailed calculations of a conformational pathway lead to an accumulation of a huge amount of data, in sharp contrast with the experimental studies, which give only a limited number of activation parameters like the activation free energy ($\Delta G^{\#}$), the activation free enthalpy ($\Delta H^{\#}$), and activation free entropy ($\Delta S^{\#}$) changes. A possible way to link the results of experiments and calculations is using site-directed mutagenesis.

In this study we characterize a more limited folding problem, experimentally by Fluorescence Stopped Flow (FSF) measurements as well as by the TMD method (Schlitter et

Reprint requests to: Yves Engelborghs, Laboratory of Biomolecular Dynamics, Katholieke Universiteit Leuven, Celestijnenlaan 200D, B-3001 Leuven, Belgium; e-mail: Yves.Engelborghs@fys.kuleuven.ac.be; fax: +32-16-327-974.

[3]Present address: Innogenetics, Industriepark Zwijnaarde 7, Box 4, B-9052 Ghent, Belgium.

Article and publication are at http://www.proteinscience.org/cgi/doi/10.1110/ps.04709604.

al. 1993; Swegat et al. 1997). As a model system we chose the activation of α-chymotrypsin from its inactive conformation (PDB ID: 2CGA) to its active conformation (PDB ID: 4CHA). The physiological process is characterized by the proteolytic cleavage of the R15-I16 bond and a subsequent series of loop rearrangements due to which, space is created for residue I16 to rotate into the interior of the protein and to form a stabilizing salt bridge between its amino terminus and the side chain of D194 (Wang et al. 1985; Wroblowski et al. 1997).

This conformational change was studied previously (Fersht and Requena 1971) using the binding of proflavin to the active site. Here we show that this conformational change can also be followed by measuring the protein fluorescence. The conformational change from the active into the inactive form is induced by a pH jump from pH 11.0 to pH 6.8. The rate constants are obtained as a function of temperature and the activation parameters ($\Delta G^{\#}$, $\Delta H^{\#}$, $\Delta S^{\#}$) are determined consequently.

Several mutants were made to challenge the conformational pathway that was previously simulated by TMD for the activation process of the bovine wild-type α-chymotrypsine (bWT; Wroblowski et al. 1997). Knowing from modeling the main structural features and events of the bWT activation, mutational loci and suggestions for the mutation types were made. Based on the type and the location of the mutations, predictions on the mutational effect on the kinetics of activation, that is, accelerating or decelerating, were done. These predictions were checked by FSF measurements carried out for each mutant. Interestingly, the results and the preliminary assumptions did not match in all cases. Therefore, to elucidate the discrepancies, further MD and TMD calculations will have to be carried out on each of these mutants.

Results

Wild-type protein and mutants

The activation process of the following chymotrypsin variants were analyzed: wild-type bovine-chymotrypsine (bWT), Δα-rat-chymotrypsine (WT), and mutants of the WT. Figure 1 indicates the locations of the mutation sites, and Table 1 shows the type of mutations and their assumed effects on the activation kinetics. Making our predictions we took the simple reasoning that less bulky residue being introduced into segment2 (sg2; Fig. 1) at position N18 (Wang et al. 1985; Wroblowski et al. 1997) would facilitate the rotation of residue I16 by reducing the rigidity of sg2 in the case of mutant N18G, while more bulky and rigid residues replacing V17 and G19 would have the opposite effect (mutants V17P and G19V). Mutations G187V, S217G, G218V, and S223A are located behind the cleft into which residue I16 rotates, in loops that rearrange upon activation. These residues undergo significant dihedral angle switches during activation, and were identified as hinge regions (G. Verheyden, J. Mátrai, P. Krüger, and Y. Engelborghs, unpubl.) for loop and segment motions that accompany the rotation of sg2. We expect that more bulky residues introduced into

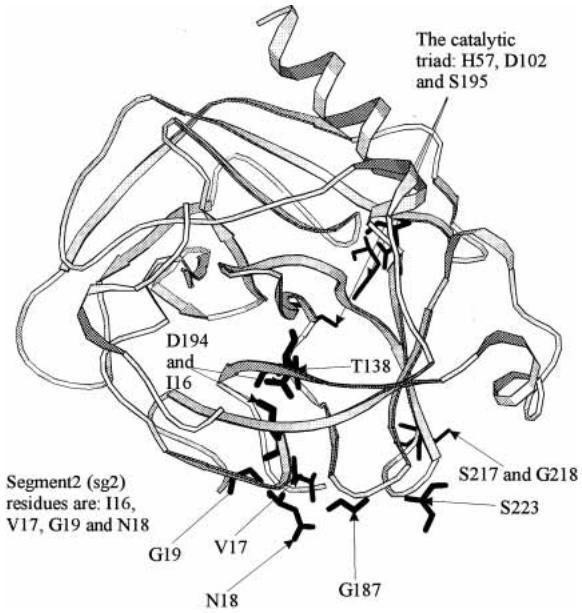

Figure 1. Schematic representation of the mutation places and the catalytic triad (black rods). Figure was made from the 4CHA PDB file.

Table 1. *The chosen mutations and their predicted effects*

Mutation	Sterical effect	Expected effect on the activation kinetics
V17P	Blocking the hinge region for I16's rotation in sg2.	Deceleration or inhibition
N18G	Reducing the rigidity of the hinge region for I16's rotation in sg2.	Acceleration
G19V	Enhancing the rigidity of the hinge region for I16's rotation in sg2.	Deceleration
T138V	Modify the motion of loops that rearrange upon I16's rotation by reducing the number of H-bonds	Deceleration
G187V	Reducing the space around the cleft into which I16 rotates.	Deceleration
S217G	Enhancing the motion of loop that shifts upon activation.	Acceleration
G218V	Reducing the motion of loop that shifts upon activation.	Deceleration
S223A	Enhancing the space around the cleft into which I16 rotates.	Acceleration

Table 2. K_M *values for the bWT, WT, and mutant enzymes*

Enzyme	K_M (μM)	Standard deviation K_M (μM)
bWT	82	15
WT	49	18
V17P	75	24
N18G	51	14
G19V	81	7
T138V	92	23
G187V	32	6
S217G	61	3
G218V	53	11
S223A	34	8

these sites appear as obstacles for the rotation of I16 and as hindrances of loop reorganization, while smaller ones enlarge the space around sg2 and so facilitate I16's rotation and the loop movements. By making our proposals about the effect of mutations on the activation kinetics, we also took into account that the removal or the introduction of potential H-bridge donor residues at the hinge regions would decrease or increase the number of H-bonds that have to be broken upon transition and so facilitate or retard the activation. Consequently, regarding both the sterical and H-bonding criteria we propose that mutation N18G, S217G, and S223A would cause acceleration while mutation V17P, G19V, G187V, and G218V would result in deceleration of the activation process compared to the WT. In the case of mutant T138V, the motion of loops and strands that rearrange upon I16 rotation is modified by reducing the number of H-bonds in the β-barrel in which residue T138 can be found. This residue is not located in a hinge region but in an extended β-sheet environment. Therefore, we suppose that the disruption in the regular H-bond network of the β-barrel caused by the mutation causes retardation in the motion upon activation of the rearranging β-barrel's strands and in the linked loop movements, and so results in deceleration of the activation.

In the case of each mutant it was checked and verified that they are sterically realizable. The choice for rat-chymotrypsin (WT) instead of the bovine variant in the preparation of the mutants was due to the availability of the rat gene sequence in contrast to the bovine variant and because of cloning and purification reasons (Verheyden et al. 2000). The role of the α-propeptide is discussed elsewhere (G. Verheyden, J. Mátrai, P. Krüger, and Y. Engelborghs, unpubl.).

Our goal with the choice of the mutations was to alter the pathway of the activation process, preferentially without altering the final state. The quality of the final state was assessed by measuring the K_M values of each mutant (Table 2). The Michaelis constants for each variant were in the range of 32–92 μM, which is in good agreement with the 31–91-μM range found in the literature (Delmar et al. 1979; Brothers and Kostic 1990; Hedstrom et al. 1994; Venekei et al. 1996a). Consequently, it can be concluded that the active site and substrate-binding pocket did not undergo substantial conformational deformation due to the introduced mutations.

The active state of the enzymes was also checked by their absorption and fluorescence emission spectra (Fig. 2A,B) and by a succinyl-AAPF-pNA-hydrolysis test. It is known that the characteristic shoulder at 295 nm in the absorption spectra of the native chymotrypsin disappears if the enzyme denatures (Fig. 2A). In the emission spectra a red shift of the emission maximum can be seen upon denaturation (Fig. 2B). The denatured enzymes show no activity in the succinyl-AAPF-pNA-hydrolysis test. All these controls verified that the enzymes were in their native active form after the purification processes. Excitation was done at 280 nm, and the pH was kept constant at 6.8.

Stopped-flow experiments

Tryptophan fluorescence spectroscopy can be used to follow the activation process of the Δα-Chymotrypsin due to

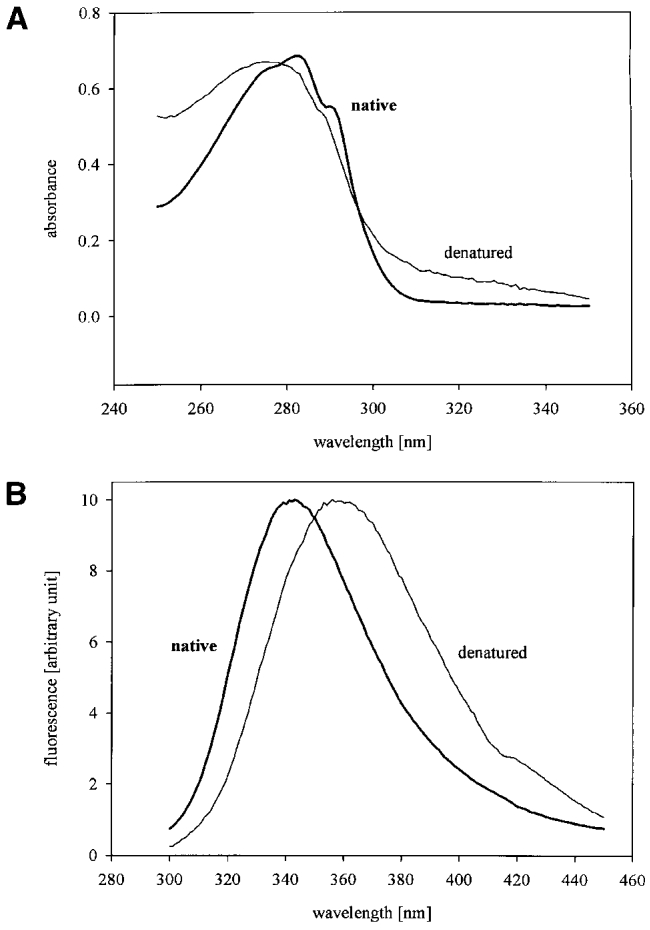

Figure 2. Absorption spectra (*A*) and normalized fluorescence-emission spectra (*B*) at excitation wavelength = 280 nm of the native and denatured chymotrypsin structures at pH 6.8.

the sensitivity of tryptophan as a fluorescence probe toward the changes in its environment. In chymotrypsin 8 tryptophan residues are present. Their contribution to the total protein fluorescence and mutual energy transfer was characterized before (Desie et al. 1986). A significant increase in the fluorescence intensity of Δα-Chymotrypsin (excitation at 280 nm) can be seen due to the conformational change from the inactive (pH 11.0) into the active conformation (pH 6.8 [Fig. 3]). Based on this signal the characteristic kinetic constant (k_{obs}) values were determined in the stopped flow measurements as explained in Materials and Methods. For all variants the process follows first-order kinetics, and can be described by equations 1 and 2:

$$E_I \underset{k_{-1}}{\overset{k_1}{\rightleftarrows}} E_A \text{ and } k_{obs} = k_1 + k_{-1} \ (\approx k_1) \quad (1)$$

where E_I = chymotrypsin in the inactive conformation, E_A = chymotrypsin in the active conformation, k_1 = activation rate constant (sec^{-1}), k_{-1} = inactivation rate constant (sec^{-1}), and k_{obs} = observed rate constant (sec^{-1}).

$$f = A + Be^{(-k_{obs}t)} \quad (2)$$

where f = the fluorescence signal in arbitrarily scaled units, A = the limiting value at $t = \infty$, B = the amplitude, k_{obs} = the observed rate constant (sec^{-1}), and t = time (sec).

At 25°C we measured the value of 2.5 ± 0.2 sec^{-1} for the kinetic constant of the WT bovine-chymotrypsin, which is in good agreement with the 3.0 ± 0.3 sec^{-1} value measured previously by Fersht and Requena by using the signal due to proflavine binding in the active site (Fersht and Requena 1971).

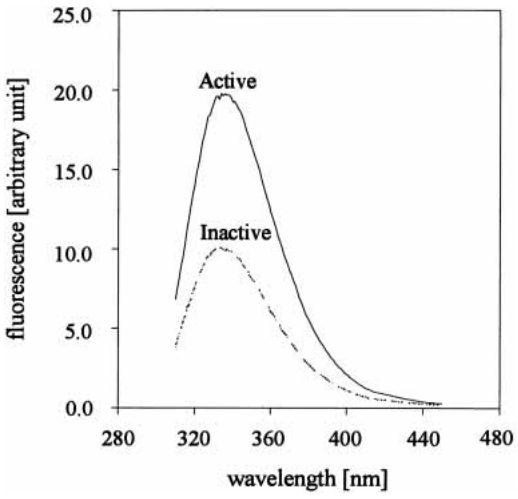

Figure 3. Fluorescence-emission spectra (excitation wavelength = 280 nm) of the active (pH 6.8, solid line) and the inactive (pH 11.0, dashed line) forms of chymotrypsin.

The differences among the kinetic constants observed for the different mutants can be attributed only to the effect of the mutations on the kinetics of activation and not to other events possibly occurring during activation, as verified by the control measurements. These events can be thermal denaturing or autocatalysis that can be triggered by sudden change in the pH as well. The control stopped-flow experiments with chymotrypsinogen and with the denatured protein samples were done in the same circumstances. No change in the fluorescence signal was observed in any of the cases. The results obtained for chymotrypsin were also concentration independent because the same values were measured with different enzyme concentrations between 4 and 40 μM.

The rate-constant values measured at different temperatures can be found in Appendix 1. It can be concluded that the mutation in case of mutants V17P, N18G, and G218V causes acceleration, while in the mutants T138V, G187V, S217G, and S223A deceleration of the activation process compared to the WT. No fluorescence signal change could be measured for several minutes for the mutant G19V, indicating the absence of an activation process and thus the inhibiting effect of this mutation. Comparing these results with the preliminary assumptions given in Table 1, it can be seen that in case of mutant V17P, S217G, G218V, and S223A our presumptions about their effect on the activation kinetics were not verified by the measurements. Thus, the concept based on sterical features and H-bonding capacities of the introduced mutations is not sufficient to explain the effect of mutations, especially when a mutation did not occur in sg2 but in more distant loops and segments. Further and more detailed analysis of the ground state and transition state stability, of the activation enthalpy and entropy change is therefore necessary to be carried out to reveal other effects of the mutations on the activation reaction.

Using the transition-state theory it is possible to calculate the activation enthalpy and entropy changes of the activation reactions from the measured kinetic rate constants. For our calculations we used the following equations:

$$k = (k_B T/h)\exp(-\Delta G^{\#}/RT) \quad (3)$$

and

$$\Delta G^{\#} = \Delta H^{\#} - T\Delta S^{\#} \quad (4)$$

and from equations 3 and 4

$k = (k_B T/h)\exp(\Delta S^{\#}/R)\exp(-\Delta H^{\#}/RT)$, from which:

$\ln k - \ln(k_B T/h) = (-\Delta H^{\#}/R)T^{-1} + \Delta S^{\#}/R$ where:

k = rate constant at T temperature [s^{-1}]

k_B = Boltzmann constant [1.381 * 10^{-23} J/K]

T = temperature [K]
h = Planck constant [6.6262 * 10^{-34} Js]
$\Delta G^{\#}$ = activation free energy change
$\Delta S^{\#}$ = activation entropy change
$\Delta H^{\#}$ = activation enthalpy change
R = the ideal gas constant [8.314 $J.mole^{-1}.K^{-1}$]

Figure 4 gives a schematic representation of the $\Delta H^{\#}$ and $\Delta S^{\#}$ values. The numerical data are summarized in Appendix 2. It can be seen that the mutations cause changes in both the enthalpy and entropy terms. Except for mutant T138V, which is the only mutant with negative $\Delta S^{\#}$ values, the transition state of the enzyme activation reaction is entropically more favorable compared to the inactive ground-state form. Thinking in the term of enzyme structure, these results imply that in all cases except mutant T138V, the transition state structure fluctuates more intensively and more wide-ranging over the whole protein structure than in the inactive ground state.

Discussion

The fluorescence stopped-flow studies performed here on the bWT, WT chymotrypsin, and on several mutants allowed us to determine with good precision the activation parameters of the process. Using the protein fluorescence the same kinetic parameters were obtained for the bWT as by looking at the binding of proflavine (Fersht and Requena 1971). This protein fluorescence-based approach has several advantages compared to the proflavine technique. The measured fluorescence intensities and so the kinetic rate constants are in direct relation with the conformational changes that take place during activation as the activation reaction follows first-order kinetics. Contrary, using the proflavin binding technique the measured rate constant is a function of the proflavin concentration. Therefore, to accurately determine the rate constant of the activational conformational changes many experiments with different proflavin concentration have to be done, which makes this method to require larger enzyme quantities compared to the protein fluorescence-based technique. Apart from that, the detection limit is lower in the protein fluorescence than in the proflaving binding method.

The mutations were suggested on the basis of the TMD pathway calculated for the bWT protein. The results show that it is possible to use theoretical methods such as TMD to detect residues that play an important role in the conformational changes accompanying the activation process and so to propose mutational sites to significantly alter the kinetic pathway of activation. As a consequence of these mutations, the rate constants are different for each mutant. Both activation parameters, the activation entropy and enthalpy have been altered, and for some mutants considerably.

The qualitative predictions based on the spatial properties and H-binding capacity of the introduced mutations are correct for some mutants but clearly not for all. On one hand, this can mean that the activation process in the bWT and in the other variants cannot be regarded as fully identical, and the introduced mutations express their effect in a manner different from what was expected based on the WT activation behavior. Therefore, our knowledge derived from the TMD simulations done only on the bWT might lack impor-

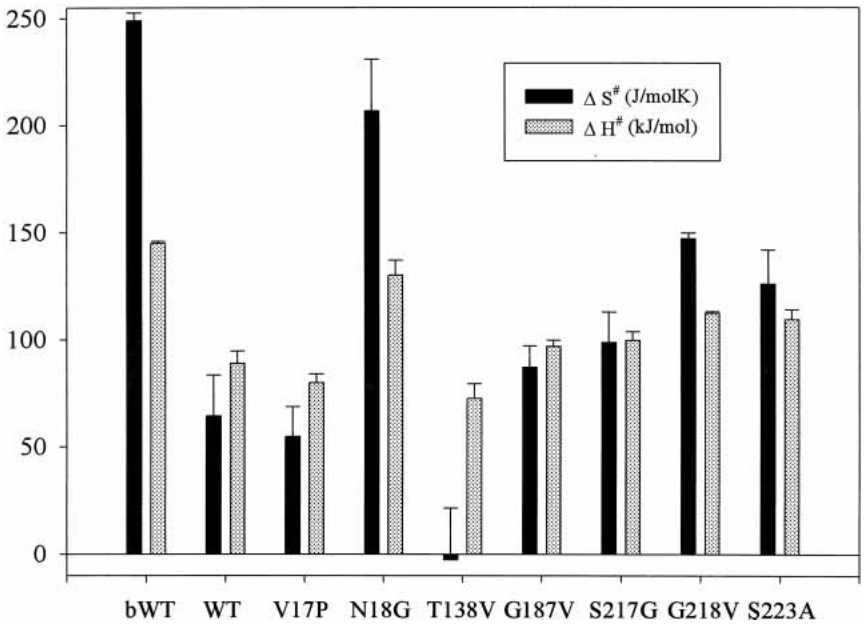

Figure 4. Schematic bar representation of the activation enthalpy, $\Delta H^{\#}$ and entropy, $\Delta S^{\#}$ values.

tant information about the activation structures and events in the mutants. On the other hand, as a reason for the discrepancies between some of our assumptions and the final results of the FSF experiments it is possible that the considered spatial and H-bonding features of the residues are not sufficient to describe all the mutational effects. Therefore, enthalpic factors that affect the stability of the inactive and transition structures by altering the H-bond network, electrostatic and van der Waals interactions, the entropic factors that are causing changes in the protein's and solvent's degrees of freedom, in the nature of protein fluctuations, should be examined in a more profound manner that covers not only the local environment of the mutational site but looks at more distant protein regions as well.

To rationalize such an in-depth analysis and to be able to compare experimental and simulation results on a wider base, MD and TMD calculations of each mutant rather than only of the bWT species will have to be performed. The dynamic behavior and so the structure and stability of the inactive and active structures of each mutants can be explored by the MD technique. The TMD method can be used to investigate structural differences caused by the mutations in the conformations sampled along the activation pathway. To estimate enthalpic and enthropic effects, to interpret and verify on a structure-related base the measured $\Delta S^{\#}$ and $\Delta H^{\#}$ values, differences in the activation H-bond pattern, in the electrostatic and van der Waals interactions, and alterations in the accessible surface area, in the fluctuation pattern, and the rotational freedom change occurring upon enzyme activation can be revealed by TMD also.

The experimental kinetic parameters presented here provide a nice set of data to test the abilities of other theoretical methods as well.

Materials and methods

Bacterial cultures

Cloning, mutagenesis, and plasmid production was done in the *Escherichia coli* WK6 strain. The desired point mutations in chymotrypsin were introduced by using inverse PCR, and the appropriate primers and verified by DNA sequencing. Production of the recombinant zymogens was performed using the yeast expression system as described for carboxypeptidase (Phillips et al. 1990). The desired α-factor leader-chymotrypsin fusion constructs were expressed in the W303-1α strain under control of the ADH-GAPDH promoter and secreted in the growth medium. In this study, mutant chymotrypsinogens were used, in which the chymotrypsin propeptide was substituted for trypsin propeptide and site Cys122 was mutated to Ser. This chimeric form of zymogen chymotrypsinogen was chosen because it was proven to be much more stable than the natural WT, and allowed activation with enterokinase (Venekei et al. 1996a,b).

For preparative purposes, 5l cultures were grown and harvested after 3 days of incubation at 30°C. Purification of the secreted recombinant protein was performed as follows: After 15 min centrifugation of the yeast culture at 10,000*g* and 4°C, the supernatant was collected and $(NH_4)_2SO_4$ was added to a final concentration of 2.4 M. Concentration and recuperation of the precipitated chymotrypsinogen was performed by 30 min centrifugation at 16,000 × *g* and 4°C. After discarding the supernatant, the obtained protein pellet was resolubilized in 20 mL buffer (50 mM Tris/HCl at pH 8.0, 0.2 M NaCl, 0.1 M $CaCl_2$). Intermediate purification of the zymogen was performed by hydrophobic interaction chromatography. Therefore, $(NH_4)_2SO_4$ was added to the protein solution to a final concentration of 1.2 M. After pH adjustment to pH 8.0 and a 0.22-μm filtration, the sample was applied at 0.5 mL/min on a HiLoad 16/10 Fenyl Sepharose column (Pharmacia) that was equilibrated with 5 column volumes of equilibration buffer (1.2 M $(NH_4)_2SO_4$, [pH 8.0]). After a washing step with equilibration buffer at 1.0 mL/min until a stable baseline was reached, the recombinant chymotrypsinogen was eluted at 1.0 mL/min using a 50 mM Tris/HCl, 20 mM $CaCl_2$ (pH 8.0) elution buffer. After pooling of the chymotrypsinogen containing protein fractions, the protein solution was dialyzed against activation buffer (50 mM Tris/HCl, 20 mM $CaCl_2$, 50 mM ε-amino-n-caproic acid [pH 8.0]), using a 12,000 MWCO dialysis membrane (Spectra/Por). Activation of the zymogen was obtained by overnight incubation at 4°C with bovine enterokinase (Boehringer) using an enzyme:substrate ratio 1:30 (w/w). To reduce autodigestion, this activation was performed at 4°C in the presence of Ca^{2+} ions and the reversible chymotrypsin inhibitor ε-amino-n-caproic acid (Chervenka 1959; Delaage et al. 1968; Steffen and Steffen 1976; Sano et al. 1988). The active chymotrypsin forms were further purified at 4°C using a XK-16 column (Pharmacia) packed with 10 mL SBTI Sepharose resin (Sigma-Aldrich) (Amneus et al. 1976; Kasche et al. 1977) in the polishing step. The protein solution was applied at 0.25 mL/min on the SBTI column, which was previously equilibrated with 5 column volumes of a 50 mM Tris/HCl, 0.2 M NaCl, 0.1 M $CaCl_2$ (pH 8.0), buffer. After application of the protein sample, the column was thoroughly washed with equilibration buffer until a stable baseline was obtained. Elution of the active chymotrypsin forms was done at 1.0 mL/min with acetic acid buffer (0.1 M HOAc at pH 4.0, 0.2 M NaCl, 0.1 M $CaCl_2$). The low pH prevents autodigestion, and the Ca^{2+} ions prevent dimerization (Aune et al. 1971; Stoesz and Lumry 1978; Shearwin and Winzor 1990). The purity of the preparates was analyzed by SDS polyacrylamide gel electrophoresis (Verheyden et al. 2000).

Protein concentration was calculated on the basis of the molar extinction coefficient of 5.104 $M^{-1} \cdot cm^{-1}$ at 280 nm (Dixon and Neurath 1957). Because in all the mutants the content of tryptophan and tyrosine residues remains the same, the same extinction coefficient is taken for the mutants as for the WT. The purified protein was concentrated when necessary by centrifugation in the Centriplus or Centricon system (cutoff 3000 Da) (Amicon) at 3000*g*.

Activity tests

Activity of the enzyme and the mutants is tested by following spectrophotometrically at 410 nm, the hydrolysis of the substrate Succinyl-Ala-Ala-Pro-Phe-p-nitroanilide (Sigma-Aldrich) (Delmar et al. 1979). The test solution is made in HEPES-buffer (50 mM HEPES, 10 mM $CaCl_2$, 100 mM NaCl [pH 8.0]) at 25°C. Substrate and product concentrations can be calculated from the O.D. at 315 and 410 nm using the respective molar extinction coefficients of 14,000 $M^{-1} \cdot cm^{-1}$ and 8400 $M^{-1} \cdot cm^{-1}$ (Delmar et al. 1979; Hedstrom et al. 1994). The K_M parameter was determined from the curve of product formation as a function of time. The

substrate was used in three different concentrations between 0.04 and 0.4 mM. The integrated Michaelis-Menten curve was used to fit the data. The corresponding equation was as follows:

$$[P] = k_{cat}[E_0]t - K_M\ln([S_0]/([S_0] - [P]))$$

where t = time, $[S_0]$ = substrate concentration at time 0, and $[P]$ = product concentration at time t. We focussed on the parameter K_M because we want to compare the ground state properties of the WT and the mutant enzymes.

Stopped-flow measurements

The conformational change that leads to the active enzyme is induced by a pH jump from pH 11.0, where the enzyme is in its inactive conformation, to pH 6.8, where the enzyme becomes active. For that purpose a volume of the chymotrypsin solution (20 μM protein and 5 mM phosphate buffer) at pH 11.0 is mixed with an equal volume of a strong buffer solution (100 mM PIPES) at pH 6.8. The conformational change is followed by measuring the increase in the protein fluorescence intensity as a function of time. As the activation reaction takes place at the millisecond time scale, the measurements were carried out in a stopped-flow instrument built in the laboratory (Lambeir and Engelborghs 1981). As excitation source a Hamamatsu 150 Watt He-Xe arch lamp (L2482) was used. The excitation wavelength was set to 280 nm, using an Oriel monochromator. The optical path length in the stopped-flow measuring chamber was 2 mm and perpendicular to the flow direction. The fluorescence was collected at 90° and passed through a cutoff filter of 300 nm (Kodak Wratten filter 2B) and was measured by a fast photomultiplier. The dead time of the instrument was approximately 2 msec, as determined by the reaction between N-bromosuccinimide and N-acetyltryptophan amide (Peterman 1979). Both reagent solutions, the mixing and measuring chambers were kept at a fixed temperature. The temperature was measured by a Fluke-51 thermometer, which was inserted into the metal thermobloc, close to the mixing chamber. The desired buffer conditions of the protein samples were assured by dialysis or, alternatively, by desalting on a PD-10 exchange column (Pharmacia). Each measurement was performed at least three times at each temperature. The experimental curves were fitted to a sum of exponentials using a home built program for nonlinear least-squares fitting based on the Marquardt algorithm (Bevington 1969). All the other fittings and analyses were done using the SigmaPlot program, version 8.0 (SPSS Inc.). To determine the standard activation enthalpy and entropy changes, measurements were carried out in the temperature range from 8 to 35°C with the intervals of 5°C.

Fluorescence spectroscopy

Fluorescence spectra of the protein samples were taken with a SPEX Fluorolog 1691 spectrofluorimeter (Spex Industries). As an excitation source, an SPEX 1907P Xenon arch lamp of 450 W was used. The slit width was 2 mm. The wavelength resolution of the excitation monochromator was 7.2 nm, with 3.6 nm for the emission monochromator. The spectra were corrected against the wavelength dependence of the emission monochromator and the photomultiplier. The excitation wavelengths were 280 and 295 nm. The emission was collected through a high-pass filter with wavelength range from 300 to 450 nm (UV-30 Hoya). The enzyme samples were at approximately 2-μM concentration.

Acknowledgments

J.M.'s work was supported by the scholarships for students from Central and Eastern Europe COE (ref. nos. OE/00/20 and OE/01/07) and the Fund for Scientific Research Flanders. G.V. was funded by the same fund. We thank Prof. W.J. Rutter (Hormone Research Institute, University of California, San Francisco, CA) for providing us the pTRAP vector with the gene of rat-Chymotrypsin.

The publication costs of this article were defrayed in part by payment of page charges. This article must therefore be hereby marked "advertisement" in accordance with 18 USC section 1734 solely to indicate this fact.

Appendix 1. *Rate constant values of the different chymotrypsin variants as the function of the temperature*

Chymotrypsine	t (°C)	k (sec^{-1})
bWT	16.4	0.434 ± 0.008
	20.9	1.070 ± 0.070
	25.0	2.50 ± 0.20
	29.4	6.10 ± 0.10
	34.3	15.0 ± 1.0
WT	11.3	0.58 ± 0.13
	15.7	0.98 ± 0.20
	20.1	2.04 ± 0.22
	25.0	3.84 ± 0.69
	28.5	4.7 ± 1.0
V17P	10.2	6.59 ± 0.64
	14.8	13.6 ± 1.3
	19.6	22.9 ± 1.9
	24.2	44.3 ± 4.8
	29.0	67 ± 13
	34.6	104 ± 26
N18G	8.7	0.30 ± 0.07
	13.5	0.60 ± 0.17
	18.3	2.04 ± 0.82
	22.1	3.90 ± 0.27
	27.4	8.9 ± 2.4
T138V	12.2	0.260 ± 0.090
	16.5	0.350 ± 0.034
	21.9	0.610 ± 0.050
	28.6	1.42 ± 0.37
G187V	7.8	0.189 ± 0.004
	10.6	0.287 ± 0.040
	15.6	0.57 ± 0.11
	20.2	0.978 ± 0.081
	24.6	2.16 ± 0.15
	30.0	4.3 ± 1.1
S217G	7.9	0.260 ± 0.070
	13.0	0.540 ± 0.020
	17.4	0.97 ± 0.12
	20.4	1.310 ± 0.020
	23.7	2.26 ± 0.21
	27.1	4.04 ± 0.72
	30.8	7.4 ± 1.0
G218V	5.9	0.25 ± 0.12
	17.3	1.72 ± 0.64
	20.5	2.97 ± 0.55
	23.9	5.0 ± 1.8
S223A	10.9	0.170 ± 0.020
	15.6	0.330 ± 0.030
	20.1	0.750 ± 0.010
	25.0	1.61 ± 0.31

Appendix 2. *Activation entropy $\Delta S^{\#}$ and enthalpy $\Delta H^{\#}$ values of the different chymotrypsin mutants*

Chymotrypsine	$\Delta S^{\#}$ ($J \cdot mole^{-1} \cdot K^{-1}$)	$\Delta H^{\#}$ ($kJ \cdot mole^{-1}$)
bWT	249 ± 4	145 ± 1
WT	64 ± 19	89 ± 6
V17P	55 ± 14	80 ± 4
N18G	207 ± 24	130 ± 7
T138V	–3 ± 24	72 ± 7
G187V	87 ± 10	97 ± 3
S217G	99 ± 14	100 ± 4
G218V	147 ± 3	112 ± 1
S223A	126 ± 16	110 ± 5

References

Amneus, H., Gabel, D., and Kasche, V. 1976. Resolution in affinity chromatography. The effect of the heterogeneity of immobilized soybean trypsin inhibitor on the separation of pancreatic proteases. *J. Chromatogr.* **120:** 391–397.

Aune, K.C., Goldsmith, L.C., and Timasheff, S.N. 1971. Dimerization of α-chymotrypsin. II. Ionic strength and temperature dependence. *Biochemistry* **10:** 1617–1622.

Berendsen, H.J.C. and Hayward, S. 2000. Collective protein dynamics in relation to function. *Curr. Opin. Struct. Biol.* **10:** 165–169.

Bevington, P.R. 1969. *Data reduction and error analysis for the physical sciences*. McGraw-Hill, New York.

Brothers, H.M. and Kostic, N.M. 1990. Catalytic activity of the serine proteases α-chymotrypsin and α-lytic protease tagged at the active-site with a (Terpyridine)Platinum(Ii) chromophore. *Biochemistry* **29:** 7468–7474.

Chervenka, C.H. 1959. Ultraviolet spectral changes related to the enzymic activity of chymotrypsin. *Biochim. Biophys. Acta* **31:** 85–95.

Delaage, M., Abita, J.P., and Lazdunski, M. 1968. Physico-chemical properties of bovine chymotrypsinogen B. A comparative study with trypsinogen and chymotrypsinogen A. *Eur. J. Biochem.* **5:** 285–293.

Delmar, E.G., Largman, C., Brodrick, J.W., and Geokas, M.C. 1979. Sensitive new substrate for chymotrypsin. *Anal. Biochem.* **99:** 316–320.

Desie, G., Boens, N., and Deschryver, F.C. 1986. Study of the time-resolved tryptophan fluorescence of crystalline α-chymotrypsin. *Biochemistry* **25:** 8301–8308.

Dixon, G.H. and Neurath, H. 1957. Acylation of the enzymatic site of Δ-chymotrypsin by esters, acid anhydrides, and acid chlorides. *J. Biol. Chem.* **225:** 1049–1059.

Fersht, A.R. and Requena, Y. 1971. Equilibrium and rate constants for the interconversion of two conformations of α-chymotrypsin. The existence of a catalytically inactive conformation at neutral pH. *J. Mol. Biol.* **60:** 279–290.

Hedstrom, L., Perona, J.J., and Rutter, W.J. 1994. Converting trypsin to chymotrypsin—Residue-172 is a substrate-specificity determinant. *Biochemistry* **33:** 8757–8763.

Izrailev, S., Stepaniants, S., Isralewitz, B., Kosztin, D., Molnar, E., Lu, H., Wriggers, W., and Schulten, K. 1998. Steered molecular dynamics. In *Computational molecular dynamics: Challenges, methods, ideas* (eds. P. Deuflhard et al.), pp. 39–65. Springer Verlag, Berlin.

Kasche, V., Amneus, H., Gabel, D., and Naslund, L. 1977. Rapid zymogen activation and isolation of serine proteases from an individual mouse pancreas by affinity chromatography: Genetical heterogeneity of chymotrypsins of *Mus musculus*. *Biochim. Biophys. Acta* **490:** 1–18.

Lambeir, A. and Engelborghs, Y. 1981. A fluorescence stopped flow study of colchicine binding to tubulin. *J. Biol. Chem.* **256:** 3279–3282.

Peterman, B.F. 1979. Measurement of the dead time of a fluorescence stopped-flow instrument. *Anal. Biochem.* **93:** 442–444.

Phillips, M.A., Fletterick, R., and Rutter, W.J. 1990. Arginine-127 stabilizes the transition-state in carboxypeptidase. *J. Biol. Chem.* **265:** 20692–20698.

Sano, M., Tsukimura, T., and Yamazaki, A. 1988. Identification of acetylcholine, histamine and serotonin receptors in the porcine dental pulp. *Showa. Shigakkai. Zasshi* **8:** 427–431.

Schlitter, J., Engels, M., Kruger, P., Jacoby, E., and Wollmer, A. 1993. Targeted molecular-dynamics simulation of conformational change—Application to the T[–]R transition in insulin. *Mol. Simul.* **10:** 291–308.

Schlitter, J., Engels, M., and Kruger, P. 1994. Targeted molecular-dynamics—A new approach for searching pathways of conformational transitions. *J. Mol. Graph.* **12:** 84–89.

Shearwin, K.E. and Winzor, D.J. 1990. Effect of calcium ion on the dimerization of α-chymotrypsin. *Biochim. Biophys. Acta* **1038:** 136–138.

Steffen, L.W. and Steffen, B.W. 1976. Improved method for measuring fibrinogen in plasma, with use of a plasmin Inhibitor. *Clin. Chem.* **22:** 381–383.

Stoesz, J.D. and Lumry, R.W. 1978. Refolding transition of α-chymotrypsin—pH and salt dependence. *Biochemistry* **17:** 3693–3699.

Swegat, W., Krueger, P., and Schlitter, J. 1997. TMD-implementation in GROMOS96, pp. 1–11.

Venekei, I., Graf, L., and Rutter, W.J. 1996a. Expression of rat chymotrypsinogen in yeast: A study on the structural and functional significance of the chymotrypsinogen propeptide. *FEBS Lett.* **379:** 139–142.

Venekei, I., Szilagyi, L., Graf, L., and Rutter, W.J. 1996b. Attempts to convert chymotrypsin to trypsin. *FEBS Lett.* **379:** 143–147.

Verheyden, G., Volckaert, G., and Engelborghs, Y. 2000. Expression of chymotrypsin(ogen) in the thioredoxin reductase deficient mutant strain of *Escherichia coli* AD494(DE3) and purification via a fusion product with a hexahistidine-tail. *J. Chromatogr. B* **737:** 213–224.

Wang, D.C., Bode, W., and Huber, R. 1985. Bovine chymotrypsinogen-A X-ray crystal-structure analysis and refinement of a new crystal form at 1.8 Å resolution. *J. Mol. Biol.* **185:** 595–624.

Wroblowski, B., Diaz, J.F., Schlitter, J., and Engelborghs, Y. 1997. Modelling pathways of α-chymotrypsin activation and deactivation. *Protein Eng.* **10:** 1163–1174.